MODEL-BASED ASSESSMENT OF REPOSITORY INDUCED EFFECTS IN THE VICINITY OF REPOSITORIES FOR SF/HLW

A. NAMHATA, C. LI, A. PAPAFOTIOU
Intera Inc., Swiss Branch
Wettingen, Switzerland
Email: anamhata@intera.com

Abstract

Repository induced effects (RIE) play an important role in the assessment of long-term safety of a deep geological repository for Spent Fuel and High-Level Waste (SF/HLW). Three categories of RIE and the associated indicators are assessed in this study. The generation of heat from SF/HLW canisters causes build-up of pore water overpressure in the repository near-field, whereas gas generation from the corrosion of waste and construction materials can lead to gas pressure buildup in the repository structures and surrounding rock. The third effect is related to the development of the Excavation Damaged Zone (EDZ) around the repository; the vertical extent of the EDZ is associated with a reduction of the lengths of radionuclide release paths through unaffected host rock. A generic RIE indicator approach presented in this study, providing a numerical framework for quantitative assessment of: (a) the general relevance of RIE for long-term safety of the repository system and, (b) the potential of the RIE indicators to discriminate between candidate repository sites. For the evaluation of the RIE, three-dimensional (3-D) models of the entire repository system as well as two-dimensional (2-D) representations at the component scale (e.g.; models of a single emplacement room). are developed. Scoping calculations are performed in support of the integration of repository-scale with component-scale analyses and the associated dimensionality reduction (3-D to 2-D) applied to the different models. To assess the RIE, probabilistic assessments can be integrated with the uncertainty of the entire ensemble of input parameters and the propagation to model predictions can be estimated in a reliable and computationally efficient manner. The generic workflow presented in this study is considered as a versatile tool for site-specific assessment of the RIE indicators in future site selection programmes.

1. INTRODUCTION

The safe disposal of Spent Fuel and High-Level Waste (SF/HLW) is one of the major challenges for the nuclear energy industry. In Switzerland, the so-called Sectoral Plan for Deep Geological Repositories ("SGT"; see also [1]) defines the regulatory framework for the site selection process. In a previous stage of the site selection process the Opalinus Clay formation was proposed as the host rock formation [2] and Jura Ost (JO), Nördlich Lägern (NL), and Zürich Nordost (ZNO) were identified as the three candidate siting regions. In the final stage of the site selection process, the proposed sites are being examined in detail and, where necessary, supplementary geological investigations will be performed. The broadened site-specific database will form the basis to select, for each of the repositories, the site for which the general license application will be prepared for. Following the specifications in the SGT a criteria-based indicator approach will be adopted to ensure a traceable implementation of the site selection process. In this context, repository induced effects, or RIE, (thermal, mechanical, gas-related and chemical impacts) represent a category of site selection criteria which have the potential for both repository types to discriminate between the candidate sites.

Past assessments of repository induced effects were conducted using simplified geological representations of the candidate sites and generic repository configurations [3–7]. The model analyses revealed that site specific aspects (e.g., local stress conditions, repository depth, thickness of the host rock, homogeneity of the host rock, tectonic overprint) may exhibit a significant impact on the safety margins associated with the mitigation of repository induced effects. Furthermore, clear evidence was found indicating that excessive abstractions of the repository configuration can mask the impact of repository induced effects on the performance of the repository system. It was concluded that a balanced appraisal is needed for both repository types, using 2-D and 3-D representations of the total repository system and of the components thereof (e.g., emplacement rooms, seal sections, shafts), which feed eventually in the phenomenological assessment of repository performance. Depending on the complexity of the assessed phenomena and processes the model-based analyses need to draw on both, probabilistic and deterministic assessments for constraining the conceptual and parametric uncertainties of the model outputs.

The overall purpose of this paper is to propose a generic workflow for the assessment of the impact of repository induced effects on the long-term performance of the repository system for SF/ HLW. Special focus is dedicated to the question, whether site specific aspects may exhibit a significant impact on the safety margins associated with the mitigation of repository-induced effects. The analyses in this paper has been carried out for a hypothetical SF/ HLW repository design in the siting region of ZNO using a semi-generic geological site model. The assessments were conducted based on simplified thermo-hydraulic (TH) problem statements to reduce the computational effort associated with the solution of the fully coupled thermo-hydraulic-mechanical (THM) problem. The entire modelling framework has been developed with the equation-of-state module EOS5 for water and hydrogen of TOUGH2 [8]. Notably, the results of this preliminary study with generic input data and preliminary repository configurations cannot be used to draw any conclusions on the suitability of the candidate siting regions for a SF/HLW repository in Switzerland.

2. INDICATOR BASED WORKFLOW

2.1. Regulatory background

The Swiss regulator [1] defines the goals, procedures, and criterial to be applied in the site selection process in Switzerland. Four criteria groups and a total of 13 criteria are defined, applying to all stages of the site selection process. The four groups are namely,

(a) Properties of host rock and the effective containment zone;
(b) Long-term stability
(c) Reliability of geological findings
(d) Engineering stability

The criterion “Repository-induced effects” were assigned to the criteria group “Long-term stability”. The regulator [1] specifies, for each of the criteria, the various “aspect(s) to be evaluated” and their corresponding “relevance for safety”. The “assessment aspects” include features of the repository configuration and interactions that are relevant to the long-term safety and engineering feasibility of a repository concept, and whose impact on long-term safety and engineering feasibility may be site specific. The site-specific evaluation of these aspects (qualitative and/or quantitative) thereby supports the discrimination between sites. According to the specifications in SFOE (2008) and in agreement with the generic appraisal in SGT – Stage 2 (see also, [9–10]), RIE can be broadly divided into three categories:

— excavation damaged zone (EDZ),
— gas effects in the host rock and in the EDZ,
— thermal effects in the host rock.

and these categories have also been judged to have the potential to discriminate between siting regions. Having identified these categories of effects, the next step is to identify RIE indicators. These are defined as calculable parameters that are measures of the magnitude or extent of a safety-relevant perturbation to the repository system caused by a RIE [11]. Each performance measure is specific to a given potentially adverse effect of RIE.

2.2. Performance measures

Each performance measure is subject to various uncertainties. The performance envelope is defined as the uncertainty range of the considered performance measure, which depends on the conceptual and parametric uncertainties associated with the input to the assessment models. Descriptions of specific performance measures used in this study are provided below.

2.2.1. Failure Potential in the intact rock (FPI)

From a long-term safety perspective, it is desirable to avoid any plastification in the host rock due to gas-induced and thermally-induced overpressures. The possibility of plastification can be assessed using the

performance measure FPI (Failure Potential in Intact rock). Assuming the applicability of the Mohr-Coulomb criterion for shear failure, the FPI index can be expressed as:

$$FPI = \frac{\tau}{\tau_{max}} \tag{1}$$

where τ is shear stress and τ_{max} is the maximum shear stress that can be accommodated by the rock without failure. τ_{max} can be obtained using:

$$\tau_{max} = \alpha + M \cdot p' \tag{2}$$

where p' is the gas-induced or thermally-induced porewater overpressure in the rock,

$$M = \frac{6\, sin\varphi'}{3 - sin\varphi'} \tag{3}$$

and

$$a = c' \cdot \frac{6\, cos\varphi'}{3 - sin\varphi'} \tag{4}$$

In this notation c' and ϕ' are the drained cohesion and friction angle of the intact rock. A graphical representation of the Mohr circle used to obtain these quantities is given in Fig. 1. The increase of porewater pressure in the host rock due to gas production or thermal expansion of the porewater will shift the Mohr circle towards low effective stress. Shear failure occurs when the Mohr circle hits the Mohr-Coulomb failure line.

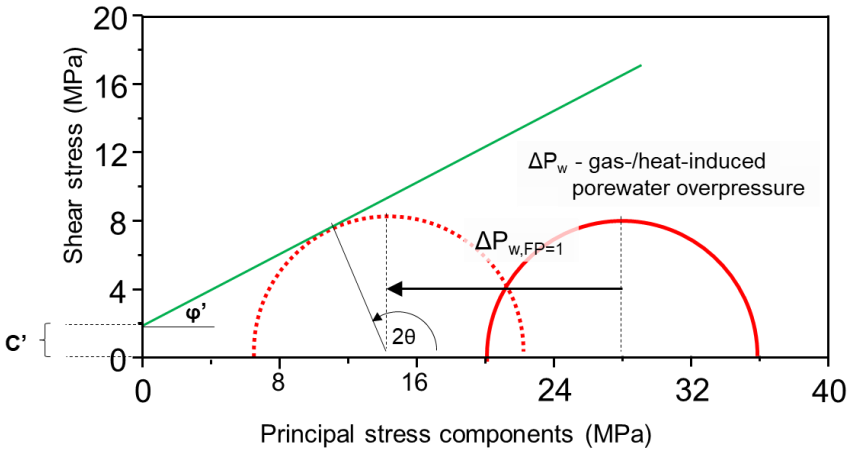

Fig. 1. Shear failure of the intact host rock in response to gas- and heat induced porewater overpressures presented as the Mohr diagram.

2.2.1. Fault Activation Potential (FAP)

Tectonic overprint in the siting regions may be associated with reduced strength of the host rock. In particular, discrete tectonic features (faults) in the host rock are often characterized by low cohesion and a low friction angle ("post-peak friction angle"). From a long-term safety perspective, it is desirable to avoid any reactivation of these faults due to overpressures. The possibility of fault activation can be assessed using the performance measure FAP (Fault Activation Potential):

$$FAP = \frac{\tau}{\tau_{max,fr}} \tag{5}$$

$\tau_{max,fr}$ is the maximum shear stress that can be accommodated by a fault without activation occurring. $\tau_{max,fr}$ is obtained using:

$\tau_{max,fr} = \alpha_{fr} + M_{fr} \cdot p'$ where M_{fr}, the post-peak friction angle, is $M_{fr} = \frac{6 \cdot sin\varphi'_{res}}{3 - sin\varphi'_{res}}$ and, assuming a cohesionless fault, $a_{fr} = 0$

A graphical representation of fault reactivation with the Mohr circle is given in Fig. 2. The increase of porewater pressure in the host rock due to gas production or thermal expansion of the porewater will shift the Mohr circle towards low effective stress. Fault activation occurs when the Mohr circle hits the Mohr-Coulomb failure line of the fault plane (no cohesion, post peak friction angle). The figure shows that fracture activation depends on the fracture orientation, which is represented by the normal vector visualized by the dip angle θfr of the fracture plane. The graph reveals that the porewater overpressures for fracture reactivation can be significantly lower than the overpressures which are needed for plastification of the intact rock.

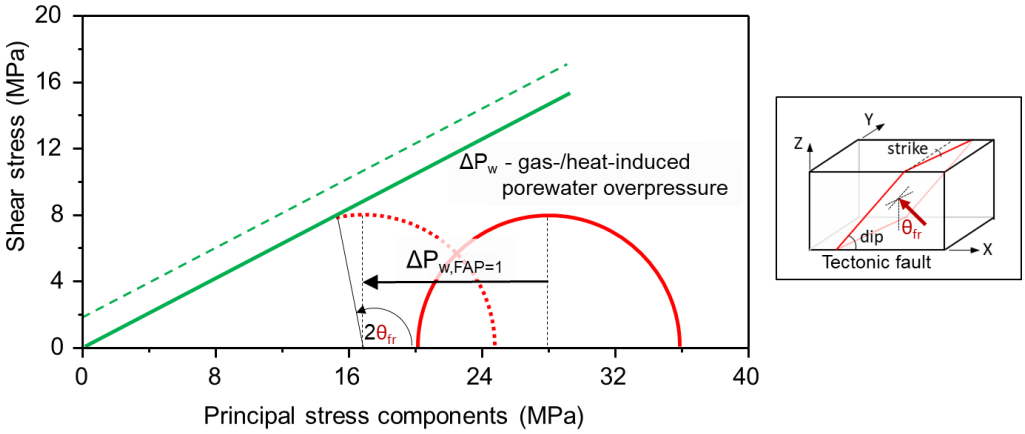

Fig. 2. Reactivation of tectonic features (faults) in response to gas- and heat induced porewater overpressures presented as a Mohr diagram.

2.2.2. Fault Leakage Potential (FLP)

In a compressive stress regime, the Opalinus Clay is characterized by a distinct self-sealing capacity. However, discrete tectonic features (faults) in the host rock may exhibit an enhanced transmissivity when the normal compressive stress on the fracture plane is reduced. From a long-term safety perspective, it is desirable to avoid a transmissivity enhancement of more than an order of magnitude in response to gas pressure build-up. However, empirical evidence and experimental results have been collected in the previous geo-synthesis report [12], indicating that a transmissivity increase of several orders of magnitude may occur, when the normal effective stress drops below 1-2 MPa (see Fig. 3).

The impact of gas induced overpressures on faults can be assessed with another performance measure, which addresses the loss of barrier function, the so-called FLP, or Fault Leakage Potential, which is expressed as:

$$FLP = \left.\frac{\sigma'_{N\,max}}{\sigma'_N}\right|_{D,S} = \left.\frac{1\,MPa}{\sigma'_N}\right|_{D,S} \tag{6}$$

where σ'_N is normal effective stress on the fault plane, $\sigma'_{N\,max}$ is the threshold **pressure** for leakage activation (based on experimental evidence from Mont Terri, a significant increase of fracture transmissivity is observed when effective normal stress on the fracture plane is less than 1 MPa) and *D* and *S* indicate dip and strike of the fault plane.

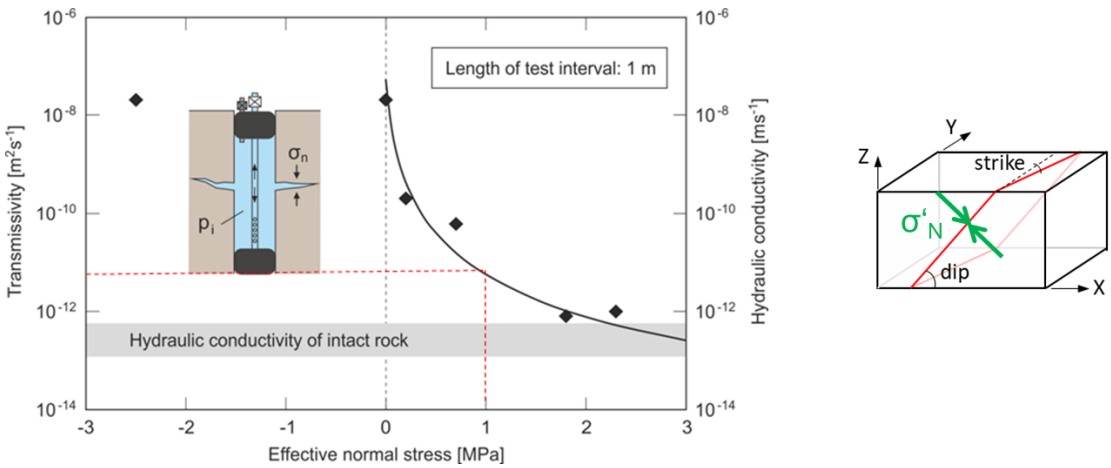

Fig. 3. Impact of variation in effective normal stress on fault transmissivity.

3. MODEL DEVELOPMENT

This section provides the model development that forms the basis for the analyses, including the introduction of the conceptual model of the SF/HLW emplacement tunnel, a brief overview of the TH models developed in TOUGH2.

3.1. Conceptual model of a SF/ HLW emplacement tunnel

In the context of SGT – Stage 2, basic layout requirements were specified for the SF/HLW repository design from the viewpoints of safety assessment and engineering feasibility. Furthermore, a generic repository layout was developed, flexible enough to cope with the different geological conditions in the proposed siting regions. Fig. 4 presents a schematic view of the generic concept for the HLW repository, displaying the main elements of the underground structures, which include: access ramp and shafts, operations- and construction tunnels, a pilot repository, emplacement tunnels for long-lived intermediate-level waste (ILW), an underground rock laboratory (URL), seal sections, and the emplacement tunnels for SF/HLW. The generic repository layout is for a waste inventory estimated based on 50 years of operation of the existing nuclear power plants. The reference distance between emplacement tunnels is 40 m.

The waste inventory includes steel canisters with spent fuel elements from the operation of nuclear power plants and vitrified HLW from the reprocessing of spent fuel. Reference dimensions of steel canisters are assuming a canister length of 4.6 m and a radius of 0.525 m. Several possible emplacement variants have been considered for the SF/HLW repository. In this paper the design variant has been used which corresponds to the reference concept for a deep SF/HLW repository as described in Nagra's technical report [13]. Waste containers are emplaced on a pedestal of compacted bentonite blocks whereas the rest of the tunnel is backfilled with compacted bentonite pellets (Fig. 4). The tunnel walls are reinforced with shotcrete lining, steel mesh and rock anchors. These ensure that the tunnels sustain the required geometry through the emplacement of waste canisters and backfilling with bentonite. SF/ HLW material properties used in this study were adopted from the preliminary database developed in SGT Stage 2. The TH properties of the Opalinus Clay were required for the simulation of heat transport through the host rock and its impact on pore pressure. Thermal properties of the host rock were taken from Johnson et al. [14] and TH calibrations of temperature profiles from deep boreholes in the candidate siting areas [15-17]. Gas-related properties of the host rock had been derived in Senger et al. [18]. Two-phase flow and associated parameterizations were described based on the assumption that the Opalinus Clay can be described as an effective homogeneous medium.

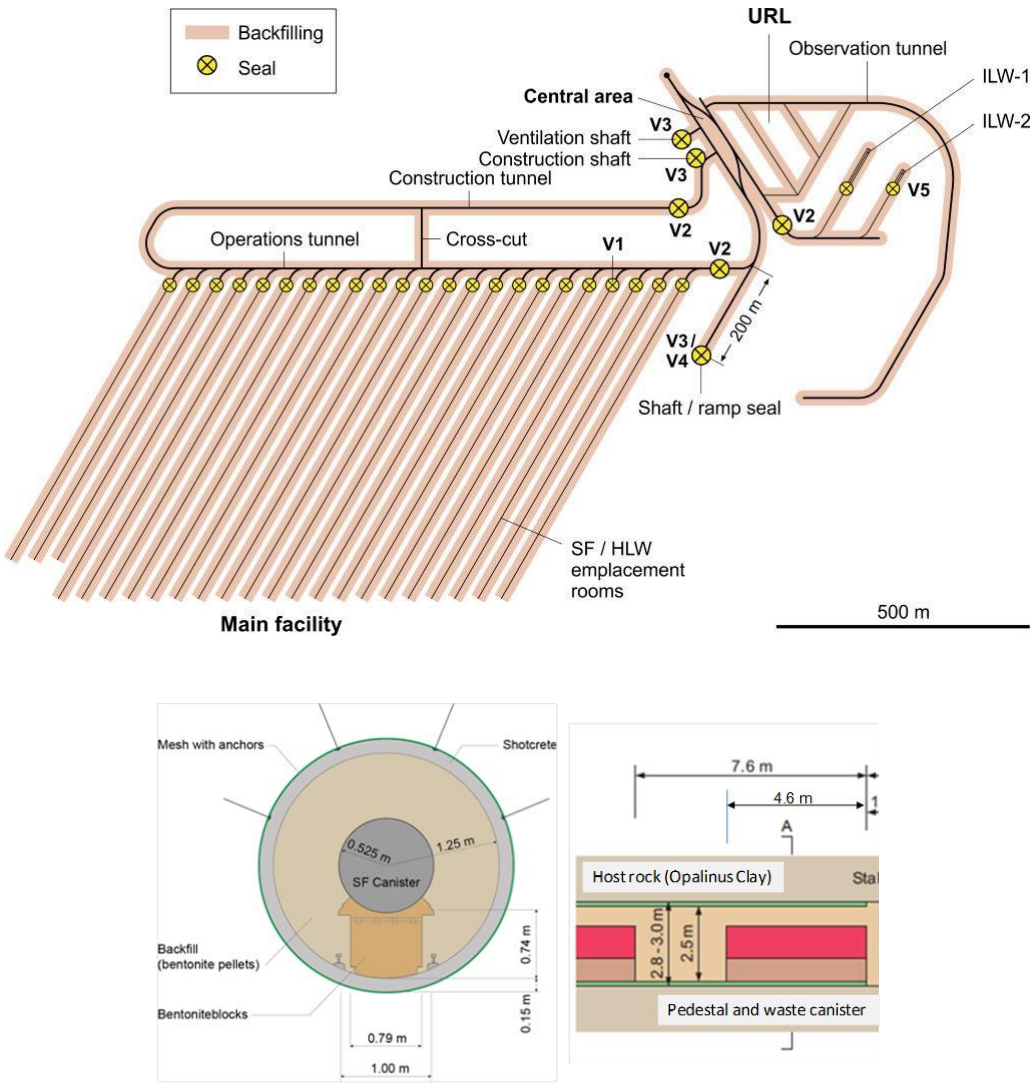

Fig. 4. Swiss HLW emplacement concept and generic design of the SF/HLW tunnels as described in Nagra (2010).

The numerical assessment models were developed based on the approach described in Papafotiou & Namhata [19]. The models were developed in two scales: repository and component. The repository scale model comprised of three-dimensional (3-D) design of the entire repository. On component scale, two model variants were developed. The first model represents cross-sections of the entire emplacement field and the other model comprises of the detailed representation of a single emplacement room. Each of these models are described in the following section. It should be noted that the models do not represent the exact repository configurations and has been developed for preliminary assessment purposes.

3.2. Development of SF/ HLW repository model

On the repository scale, the simulations are developed using the 3-D model from Papafotiou & Namhata [19] that describes the generic configuration of a SF/HLW repository (Fig. 5), considering the combined effect of heat emission and gas accumulation. The model is built upon an Integrated Finite Differences (IFD) Voronoi grid with nested refinements in the vertical and horizontal direction. The nested grid allows for a finer discretization around the repository elements that coarsens away from the repository and towards the model boundaries.

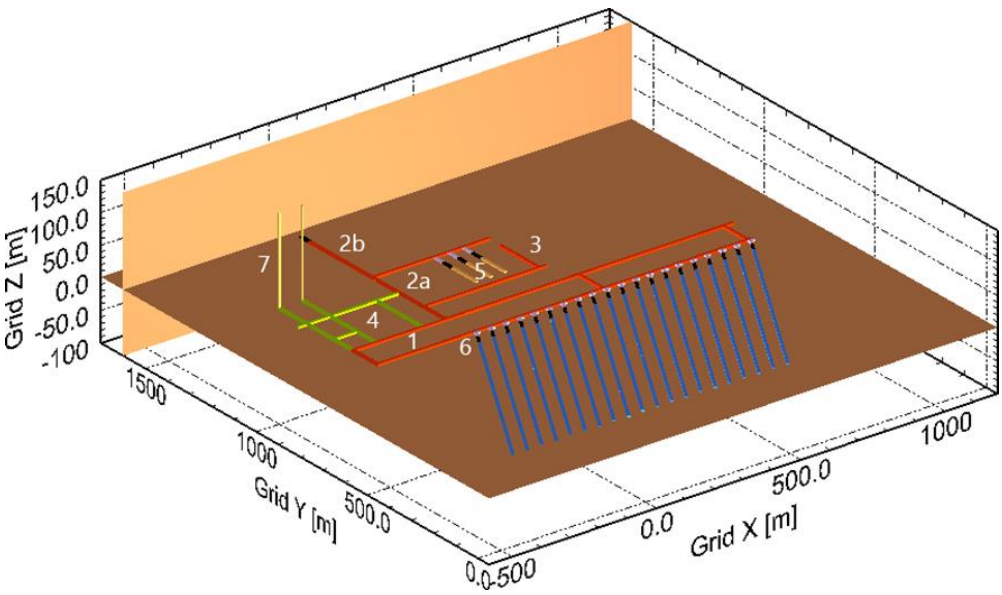

Fig. 5. Schematic 3-D representation of the SF/HLW repository model geometry with the various underground structures (ZNO); (1) operations gallery; (2a) central area; (2b) access tunnel; (3) observation gallery; (4) test facility; (5) pilot tunnels; (6) branch tunnels; (7) shafts.

The SF/HLW repository is implemented in the IFD grid as stylized representations of the different repository components that are assigned effective thermo-hydraulic properties and volumes. The repository tunnels represented explicitly in the model comprise the access tunnel to the main repository (including the central area), the access tunnel to the pilot repository, 3 pilot emplacement tunnels (corresponding in total to the length and volume of one SF emplacement tunnel) with branch tunnels and the pilot operation tunnel, 2 vertical shafts extending to the top boundary of the model, the operations gallery and parallel to it the ventilation tunnel, 2 tunnels connecting the operation gallery with the ventilation tunnel, the test facility with the observation gallery, 3 HLW emplacement tunnels, and 17 SF emplacement tunnels. Plugs and seals are placed at the entrance of emplacement tunnels (V5), the entrance of operation and ventilation tunnels (V2), and at the end of the access tunnels (V4).

The repository tunnels are inclined along the dip of the Opalinus Clay but positioning of the repository may result in some differences in the distances between the repository tunnels and the top/bottom of the host rock. Positioning of the repository has been selected such that the emplacement tunnels are located approximately in the middle of the Opalinus Clay. Porosity and heat capacity of the repository structures has been scaled to account for the volumes available for gas and heat storage. Additional information on the geometry of the individual repository elements and the volume scaling is given in Papafotiou & Namhata [19]. In this paper, the 3-D modeling results have not been shown and the model has just been used to show the derivation of the 2-D cross-section of the “ensemble” model described in the next section.

3.3. Development of SF/ HLW component scale model

3.3.1. 2-D “ensemble” model

On the component scale, the simulations are developed using two model variants namely, the “ensemble” model and the “single-tunnel” model. The first group of 2-D component models represent cross-sections of the entire emplacement field (“ensemble” models) developed based on the geometries and coordinates used in the 3-D repository models. The ensemble models comprise twenty SF/HLW drifts located in the Opalinus Clay according to the preliminary site-specific configurations. The positioning of the drifts in the Opalinus Clay is extracted from the 3-D repository models (Fig. 6) and therefore depends on the repository configuration (i.e. placement and orientation in the 3-D geological space). Fig. 7 shows the ensemble model developed for cross-section Y1 for SF/HLW tunnels located in the middle of the Opalinus Clay in ZNO. The horizontal length of the model equals 2500 m whereas the vertical extent corresponds to the Opalinus Clay layer at the selected cross-section. The spacing between the tunnel axes of the drifts corresponds to 40 m. A progressive mesh refinement

based on a Voronoi meshing is used inside and around the twenty drifts to represent the individual tunnel material components in detail (see Fig. 7). The width of the 2-D cross section is set to 1.65 m, which corresponds to the ratio between the typical canister length (4.6 m) plus the bentonite section between adjacent canisters and the canister length [20]. More details on the mesh and material properties assigned in the model are given in Papafotiou & Namhata [19].

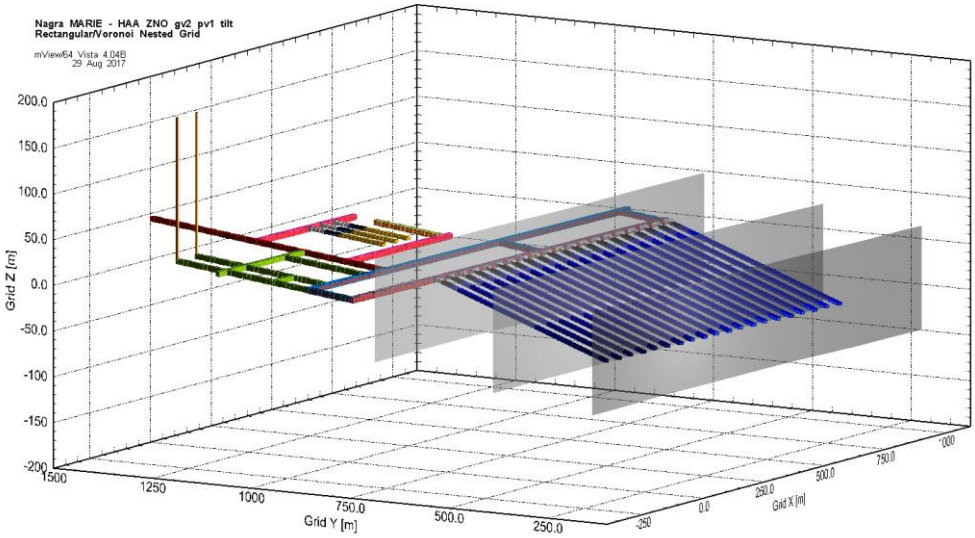

Fig. 6. 3-D view of SF/HLW repository structures in ZNO including the cross-sections Y1, Y2, and Y3 at the middle, begin, and end of the emplacement drifts, respectively.

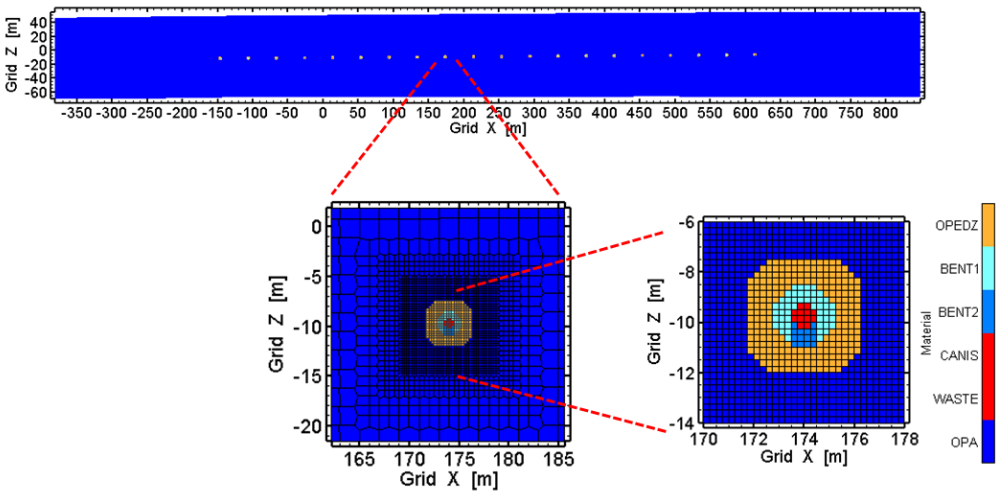

Fig. 7. Model domain (top) and Voronoi representation (bottom) of SF/HLW tunnels in the central-axis model for ZNO (cross-section Y1).

3.3.2. 2-D "single-tunnel" model ("detailed tunnel")

The second group of 2-D component models represent half emplacement room with the surrounding host rock, the so called "single-tunnel" models. The model is implemented with an IFD mesh with nested gridding near the emplacement tunnel allowing a detailed representation of the SF/HLW canister and surrounding bentonite buffer materials (Fig. 8). The lateral extent is given by the symmetry axis through the SF/HLW tunnel and the half-distance between two adjacent SF/HLW tunnels that is equal to 20 m. The vertical extent above and below the centre of the SF/HLW tunnel is adjusted accordingly for each site and consistently with the ensemble

models. The width of the 2-D cross section is set to 1.65 m. To represent the reduced length of the canister, the interface area between the canister and the surrounding bentonite is based on a 1-m width.

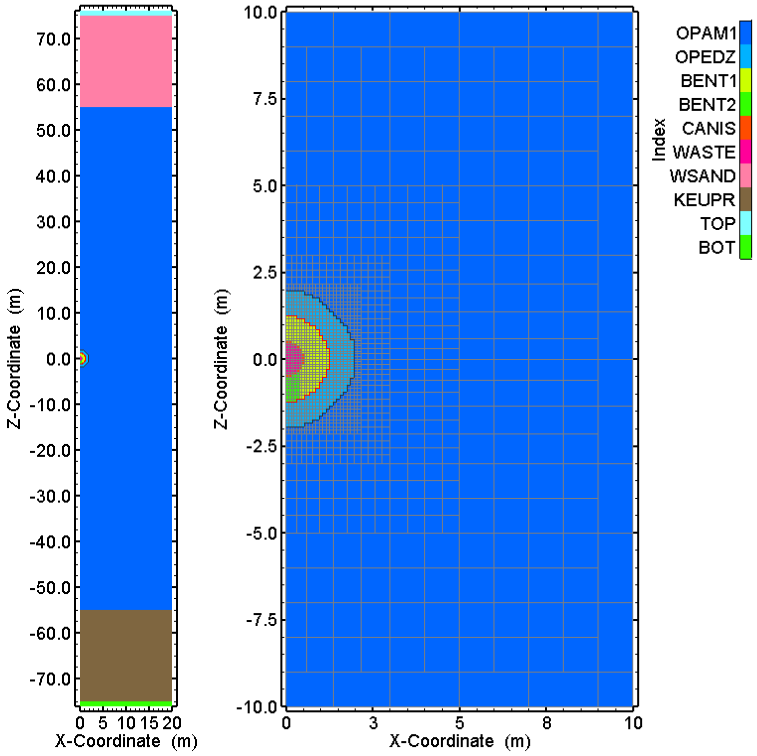

Fig. 8. Implementation of SF/HLW emplacement tunnels in the 2-D nested rectangular grid of the "single-tunnel" model.

3.4. Source terms

Source terms have been defined to estimate the amount of heat production due to radioactive decay of radionuclides in SF/HLW, as well as the amount of gas formed by the anaerobic corrosion of the SF/ HLW canisters, and corrosion of construction materials.

3.4.1. Gas generation rates

In sensitivity analyses performed in the context of SGT – Stage 2, simplistic approximations of gas generation rates (Fig. 9) were provided as reference, upper and lower bounding values. The reference gas generation rates were given as m^3-gas/Tunnel Meter/year as [6, 21]:

— gas from corrosion of SF/HLW canisters: 0.01 m^3/tm/a; until 60 000 years;
— gas from corrosion of tunnel support materials: 0.06 m^3/m/a; until 2000 years.

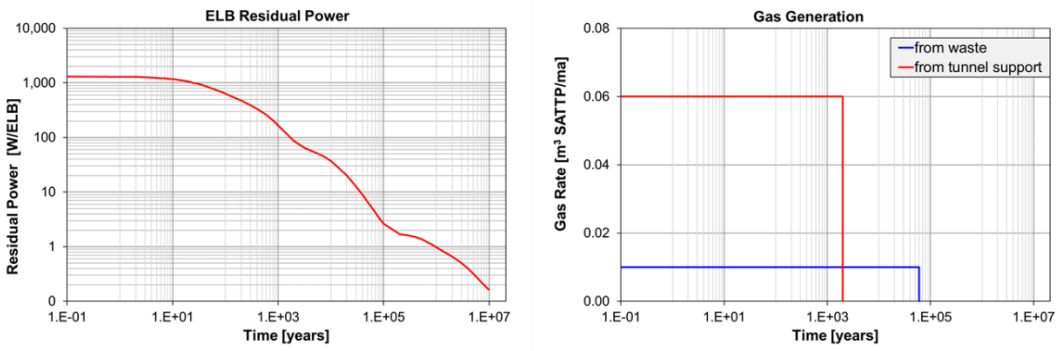

Fig. 9. Generic average heat production for SF/ HLW (left) and gas production (right) per canister as a function of time.

3.4.2. Heat generation rates

Heat generation from the radioactive decay of the waste were estimated for different waste types based on Nagra's inventory developed for the preliminary assessments of SGT Stage 2 [22]. The present analysis adopted the reference heat generation rates for a MOX/UO_2 canister, which had the highest output in the inventory (Fig. 9).

3.5. Initial and boundary conditions

The model domains (both 2-D and 3-D) are assumed to be initially fully water-saturated and hydrostatic pressures are assigned to the nodes prior to the repository construction. The top and bottom layers of the grids are connected to external boundary elements with prescribed hydrostatic pressures corresponding to conductive sub-units of the upper and lower confining units. The initial pressure distribution and the prescribed pressures at the top and bottom boundaries are adjusted depending on the desired repository depth corresponding to each site. For siting region ZNO, repository depth of 600 m below ground level is prescribed.

Accordingly, the initial temperature distribution and prescribed temperature at the top and bottom boundaries correspond to the steady-state temperature distribution based on a geothermal gradient of 0.043°C/m and a prescribed temperature of 10°C at near-surface groundwater. All vertical model boundaries represent no-flow boundaries.

Additional pressure boundary conditions are assigned to the repository ramp after the repository is sealed (post-closure period). The prescribed pressure values correspond to hydrostatic pressure at the top of the Opalinus Clay host rock.

Internal boundary conditions are assigned to open tunnels during the ventilation period through prescribed atmospheric pressure and a capillary suction corresponding to relative humidity of 60% and a tunnel temperature of 28°C. The emplacement saturation of all the backfill and seal materials is assumed to be 50%.

4. RESULTS

4.1. 2-D "ensemble" models

The 2-D "ensemble" models are used to perform base-case simulations for each repository configuration for SF/HLW based on the boundary conditions and gas and heat generation rates discussed previously (see Section 3). Due to the computational demand of these models, the simulation variants are developed in a deterministic manner with simplifying assumptions. The deterministic variants can provide spatial distributions of the FPI (Failure Potential in Intact rock) associated with the development of gas- and thermally-induced overpressures in the host rock.

The pressure time-histories simulated with the SF/HLW "ensemble" models are shown in Fig. 10. Pressure is shown at two locations, namely inside the SF/HLW tunnel and in the Opalinus Clay at 20 m distance above the tunnel. The simulated pressures show a typical evolution with an early peak associated with thermal effects after approximately 100 years followed by a second peak after 30 000 years due to gas accumulation. Spatial distributions of thermally-induced pressures after 100 years are shown in Fig. 11(a). Spatial distributions of gas-induced pressures after 30 000 years are shown for the three sites in Fig. 11(b).

Thermally-induced peak pressure in the Opalinus Clay is observed above the central tunnel and corresponds to 8.7 MPa. In comparison, thermally-induced peak pressures at 20-m above the first and last tunnel of the emplacement field are lower by approximately 1 MPa owing to the lateral dissipation of heat. Peak pressure due to gas accumulation inside the central tunnel corresponds to 8.6 MPa in ZNO. In comparison, gas-induced peak pressures inside the first and last tunnel of the emplacement field are lower by approximately 0.5 MPa. It is noted that gas generation rates in the simulations presented for SF/HLW have not undergone any scaling or adjustment to account for gas release along the repository tunnels and EDZ. The estimates of gas-induced pressures presented here are therefore conservative. As discussed previously, the times and values of peak pressures also depend on the boundary conditions imposed by the over- and underlying hydrological units which are in this case not accounted for.

The stress conditions in the proposed siting regions are currently poorly established. Reliable in situ stress measurements have been made only in a couple of boreholes. For this reason, a semi-generic stress regime, S_{ref} is specified in SGT Stage 2 for the Opalinus Clay formation in candidate siting regions JO, NL and ZNO [2] is used in this study. Based on the simulated pressure distributions, spatial distributions of FPI are calculated for the semi-generic stress regime S_{ref} ($k_{0,x}$=1.30, $k_{0,y}$=0.97). The distributions of FPI after 100 and 30 000 years are shown in Figs. 12 and 13, respectively. The maximum values of the FPI after 100 years as well as after 30 000 years correspond to 0.46.

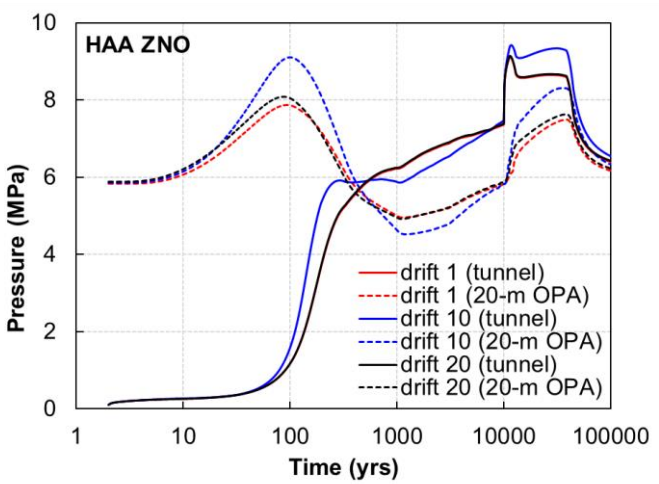

Fig. 10. Time-histories of pressure simulated with the "ensemble" models for SF/HLW in ZNO.

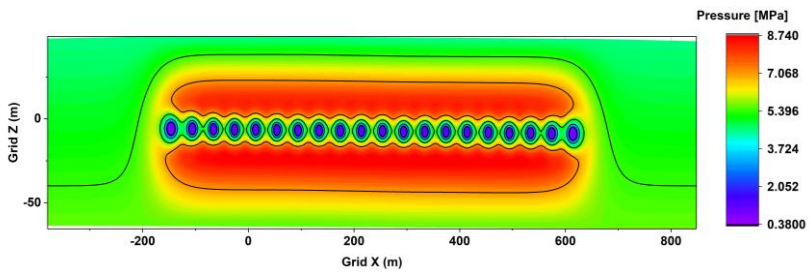

(a)

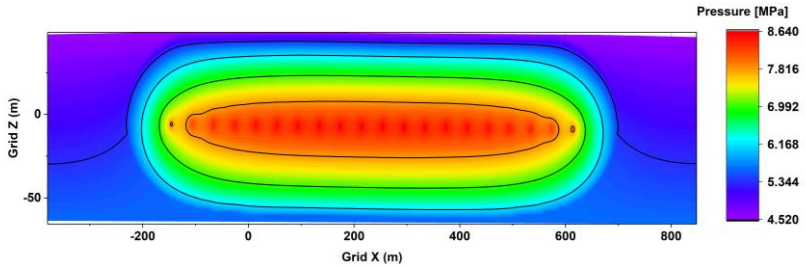

(b)

Fig. 11. Spatial plots of (a) thermally-induced pressure simulated after 100 years and (b) gas-induced pressure simulated after 30 000 years, with the "ensemble" models for SF/HLW in ZNO.

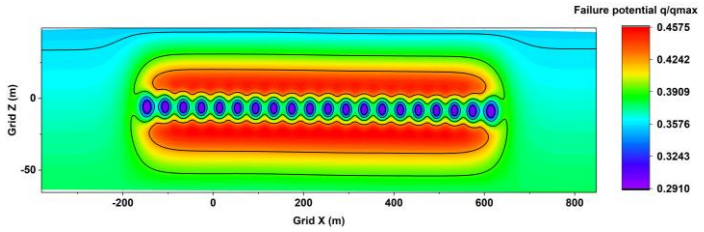

Fig. 12. Spatial distribution of FPI associated with thermally-induced overpressures in the ZNO base case for SF/HLW for stress regime corresponding to S_{ref}.

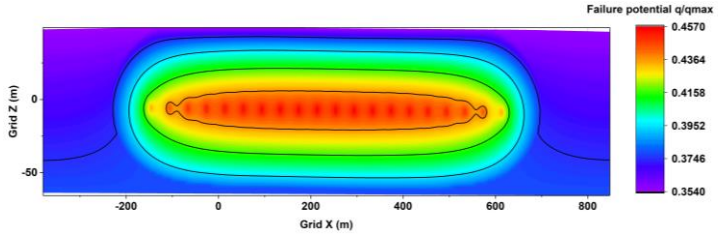

Fig. 13. Spatial distribution of FPI associated with gas-induced overpressures in the ZNO base case for SF/HLW for stress regime corresponding to S_{ref}.

4.2. 2-D "single-tunnel" model

The 2-D "single-tunnel" model is used to perform base-case simulations for each repository configuration for SF/HLW based on the boundary conditions and gas and heat generation rates discussed earlier, bracketed by uncertainty ranges associated with parametric uncertainty. The relatively low computational demand of these models allows for probabilistic assessments. The probabilistic appraisal can provide histograms of FPI associated with the expected envelopes of maximum thermally-induced overpressures in the host rock, as well as polar diagrams of the FAP (Fracture Activation Potential) and FLP (Fracture Leakage Potential) for the entire spectrum of possible fracture orientations.

The input parameters for Monte Carlo simulations are sampled from normal and log-normal distributions using latin-hypercube based on the methodology described in Papafotiou et al. [23]. The uncertain parameters selected for sampling are the absolute permeability, thermal conductivity, heat capacity and pore compressibility of the Opalinus Clay, the absolute permeability of the EDZ, the absolute permeability of the upper confining unit (UCU), and the absolute permeability and thermal conductivity of the bentonite buffer in the emplacement tunnel. The mean and standard deviations of the parameter distributions are summarized in Table 1. An overview of the resulting distributions is illustrated in Fig. 14.

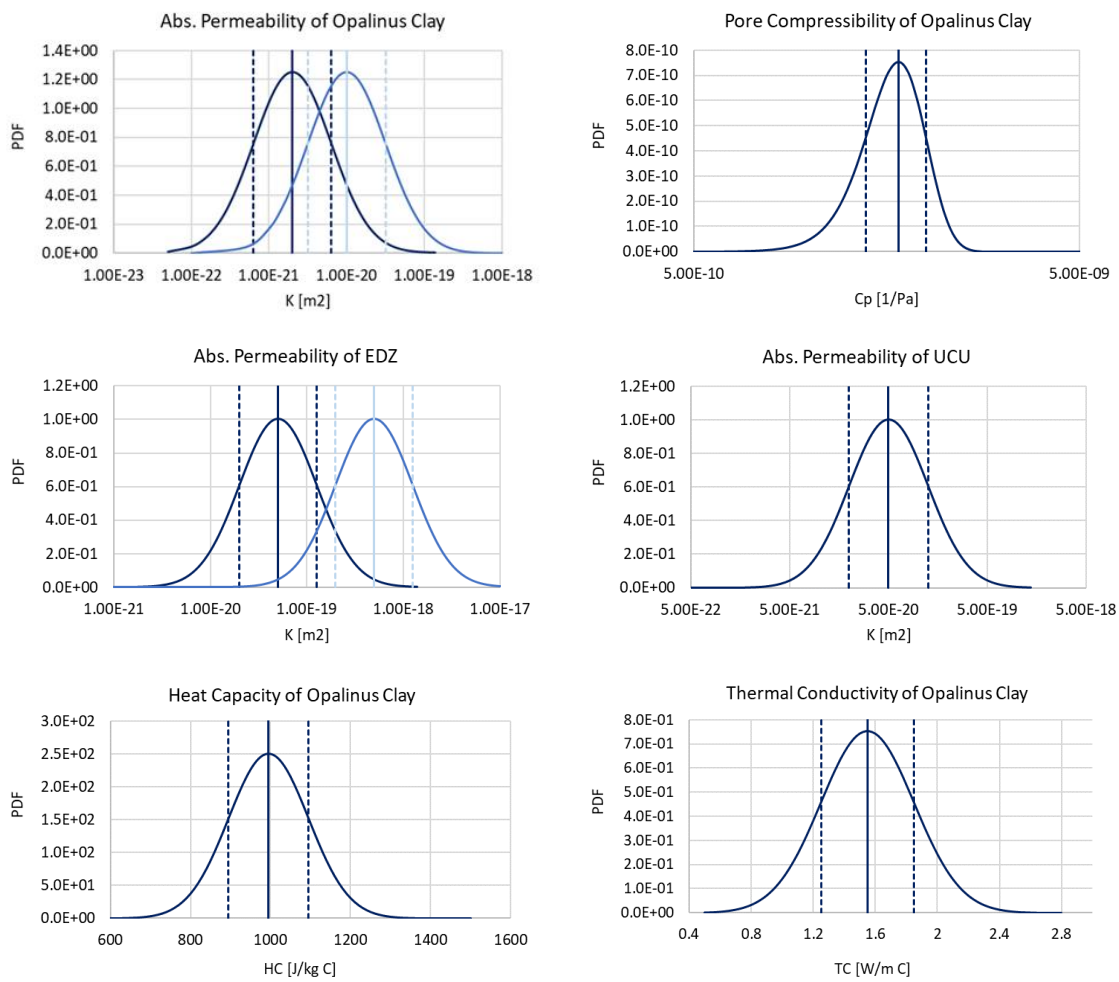

Fig. 14. Distribution of input parameters used for the Opalinus Clay, the EDZ, and the UCU in the Monte carlo simulations for the SF/HLW repository configurations (dark blue: "deep" repository; light blue: "shallow" repository; thermal conductivity shown for ZNO).

TABLE 1. REFERENCE VALUES AND STANDARD DEVIATIONS USED FOR NORMAL DISTRIBUTION SAMPLING OF THE UNCERTAIN PARAMETERS IN PROBABILISTIC ANALYSES FOR THE SF/HLW REPOSITORY.

	OPA-logK	OPA-TC	OPA-HC	OPA-Cp	EDZ-logK	UCU-logK	PELL-logK	PELL-TC
Reference	20.0	1.55	995	1.7e-9	19.3	19.3	19.5	1.0
STD	0.5	0.3	100	3.0e-10	0.4	0.4	0.3	0.15

The time-histories of temperature and pressure simulated with the SF/HLW "single-tunnel" model is shown in Fig. 15. Four locations are shown based on the earlier probabilistic analyses discussed in Papafotiou et al. [23], namely temperature at the waste canister (T1), pressure at the bentonite adjacent to the canister (P1), pressure in the host rock at 20 m distance above the tunnel (P2), and pressure at the lateral boundary corresponding to the midpoint between emplacement tunnels (P3). The dashed lines show the results of the base case simulations in each case, enveloped by the Monte Carlo simulations shown in green color (only 200 runs shown in each figure). Mean and standard deviations of the 1000 peak pressure values are shown in each plot. Peak pressure due to thermal effects in the host rock (P2) in the base case simulation is reached after approximately 800 years and corresponds to 13.1 MPa. Inside the tunnel (P1), peak pressure is equal to 13.8 MPa.

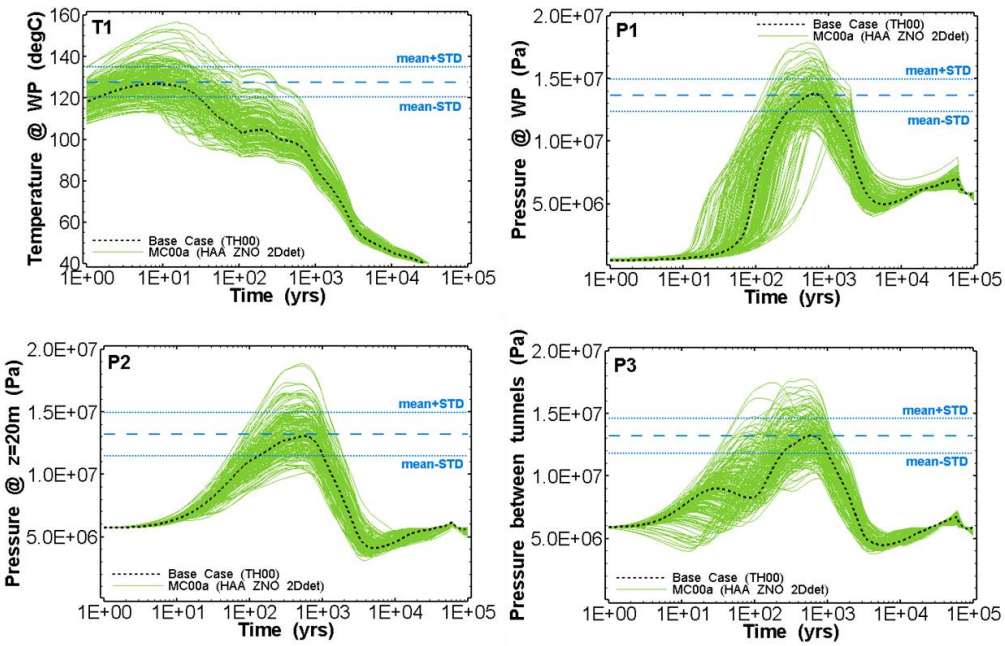

Fig. 15. Time-histories of temperature (T1) and pressure (P1, P2, P3) simulated with the SF/HLW "single-tunnel" model in ZNO base case.

Peak thermally-induced pressures simulated with the 2-D "single-tunnel" models are overall higher than the respective values obtained with the 2-D "ensemble" models due to the difference in the boundary condition. On the other hand, gas-induced pressures are lower due to the simplified gas generation rates used in the Monte Carlo simulations. In general, overpressures resulting in Mohr circle crossing the failure line result in failure of the geomechanical indicators FPI, FAP, and FLP. The number of Monte Carlo runs resulting in tensile failure in due to heat-induced effects is 179 and due to gas-induced effects is 52.

Using the 1'000 values of heat-induced peak pressure reached in the Monte Carlo simulations, histograms of FPI are calculated for the stress regime S_{ref}. The FPI histogram is shown in Fig. 16. Bins of FPI>1.0 with cumulative probability higher than 2% are shown in red. It is shown that, approximately 5% of the simulations result in FPI values between 1.0 and 1.1.

As discussed previously, indicators FAP and FLP depend on the strike and dip of the fracture. These indicators are thus presented in the form of polar diagrams covering the entire spectrum of fracture orientations in the 3-D space. For this, the heat-induced peak pressure (i.e., peak pressure in the host rock) is extracted from the "no-failure" simulations corresponding to each site to calculate the FAP and FLP in each case. Similarly, to the FPI, the indicators FAP and FLP are calculated for the stress regime S_{ref}. Fig. 17 shows the calculated average FAP associated with thermally-induced pressures for the stress regime. The FAP values reach a value of 1.0 for most configurations and fracture orientations due to the high peak pressures predicted in the 2-D simulations. In addition, the FAP associated with gas-induced pressures is shown in Fig. 17. The FAP values are overall higher but remain below 1.0. Fig. 18 shows the FLP associated with thermally-induced pressures. For S_{ref}, FLP reaches 1.0 for sub-horizontal. The FLP associated with gas-induced pressures remains below 0.5 as shown in Fig. 18.

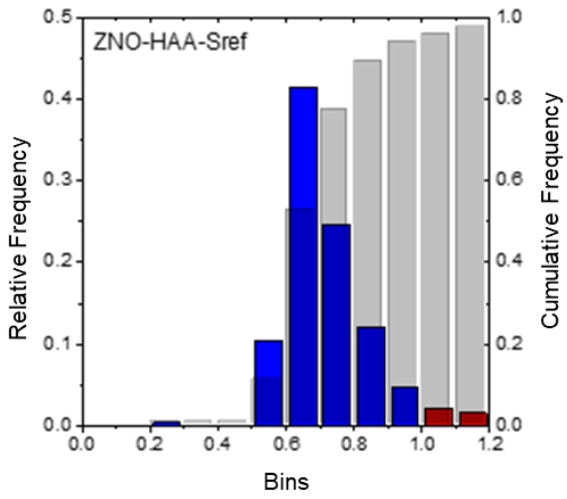

Fig. 16. Histograms of FPI in the SF/HLW repository corresponding to thermally-induced peak pressure in ZNO base case and for stress regime corresponding to S_{ref}.

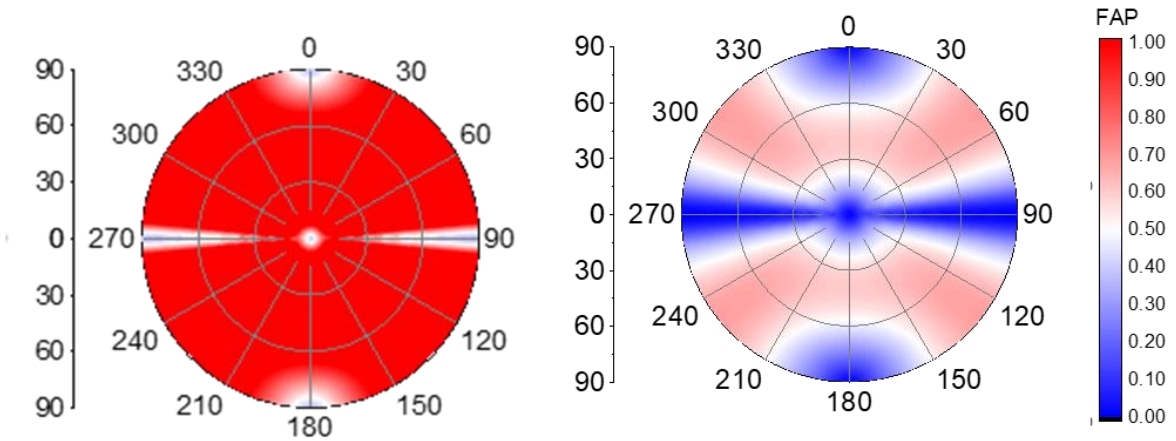

Fig. 17. Polar diagrams of FAP corresponding to maximum thermally-induced pressure (left column) and corresponding to maximum gas-induced pressure (right column) in the SF/HLW repository for stress regime corresponding to S_{ref}.

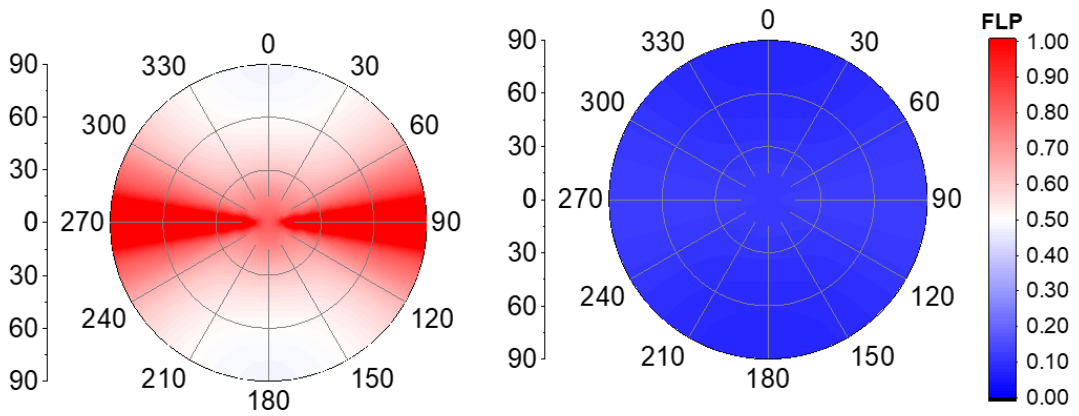

Fig. 18. Polar diagrams of FLP corresponding to maximum thermally-induced pressure (left column) and corresponding to maximum gas-induced pressure (right column) in the SF/HLW repository for stress regime corresponding to S_{ref}.

5. CONCLUSION

This paper summarizes a preliminary site-specific assessment of the repository induced effects (RIE) indicators that has been performed in the context of SF/HLW repository type. Two categories of RIE indicators were assessed in this analysis, namely the magnitude of gas-induced overpressures, and the magnitude of thermally induced overpressures. Four potentially adverse effects have been identified as being associated with these RIE, namely (i) shear failure of the intact host rock due to gas-induced or thermal overpressures, (ii) fault activation in the host rock due to gas-induced or thermal overpressures (reactivation of tectonic structures), (iii) fault leakage (enhanced transmissivity in the host rock due to gas-induced overpressures, and (iv) gas-induced displacement of pore water.

The model-based assessments have been carried out using the model portfolio described in Papafotiou & Namhata [19] developed for the evaluation of RIE. These include stylised 3-D representations of entire repository configurations integrated with more detailed 2-D representations of the entire emplacement field with the surrounding host rock as well as 2-D representations of individual repository components, namely SF/HLW emplacement tunnels. The model-based evaluations were performed using both deterministic and probabilistic appraisals. The deterministic model runs provided base-case predictions for different configurations and assumptions, which were then bracketed by predictions from probabilistic simulations. Calculatable performance measures have been defined for each of these effects, namely the Failure Potential in Intact host rock (FPI), the Fault Activation Potential (FAP), and the Fault Leakage Potential (FLP). The FPI, FAP, and FLP were assessed for gas-induced overpressures in SF/HLW configuration. The FPI and FAP were also assessed for thermally induced overpressures. In addition, assessments of FLP in relation to potentially concurrent thermally induced overpressures were provided.

The maximum values of the FPI associated with thermally-induced effects calculated in the base case for the siting region ZNO. Moreover, the maximum indicator range corresponding to cumulative probability of 5% and 20% calculated with the Monte Carlo simulations is provided. The synthesis is performed for a semi-empirical stress regime S_{ref}. The FAP and FLP are also evaluated by means of polar diagrams covering the entire spectrum of possible fracture orientations.

The RIE indicator approach applied in this paper provides a numerical framework for quantitative assessment of the general relevance of RIE for long-term safety of the repository system. The preliminary site-specific assessment of the RIE indicators presented in this paper focuses on the elaboration of a consistent and traceable workflow. Where possible, simplifying assumptions were made to facilitate the modelling workflow development (i.e. gas generation rates, boundary conditions) and allow future enhancements with site-specific configurations and data. The repository configurations, assessment models and assessment scenarios were based on the state-of-knowledge according to the reference documents of SGT Stage 2. Therefore, the results of this preliminary assessment of RIE effects are broadly consistent with the findings of SGT Stage 2 which have been described in Nagra's technical report [2].

ACKNOWLEDGEMENTS

The authors would like to acknowledge Nagra for funding this study in the framework of SGT-E3.

REFERENCES

[1] SWISS FEDERAL OFFICE OF ENERGY (SFOE), Sectoral Plan for Deep Geological Repositories, Conceptual Part. Swiss Federal Office of Energy, Bern, Switzerland, 2008.

[2] Nagra, SGT Etappe 2: Vorschlag weiter zu untersuchender geologischer Standortgebiete mit zugehörigen Standortarealen für die Oberflächenanlage. Sicherheitstechnischer Bericht zu SGT Etappe 2. Sicherheitstechnischer Vergleich und Vorschlag der in Etappe 3 weiter zu untersu-chenden geologischen Standortgebiete. Nagra Tech. Ber. NTB 14-01. Nagra, Wettingen, Switzerland, 2014.

[3] NAGRA, Effects of post-disposal gas generation in a repository for spent fuel, high-level waste and long-lived intermediate level waste sited in Opalinus Clay. Nagra Technical Report NTB 04-06, Nagra, Wettingen, Switzerland, 2004.

[4] NAGRA, Entsorgungsprogramm 2008 der Entsorgungspflichtigen. Nagra Technical Report NTB 08-01 (in German). Nagra, Wettingen, Switzerland, 2008.
[5] PAPAFOTIOU, A., SENGER, R. Sensitivity analyses of gas release from a L/ILW repository in the Opalinus Clay in the candidate siting regions of Northern Switzerland. Nagra Arb. Ber. NAB 13-92. Nagra, Wettingen, Switzerland, 2014.
[6] PAPAFOTIOU, A., SENGER, R. Sensitivity analyses of gas release from a SF/HLW repository in the Opalinus Clay in the candidate siting regions of Northern Switzerland. Nagra Arb. Ber. NAB 14-10. Nagra, Wettingen, Switzerland, 2014.
[7] PAPAFOTIOU, A., SENGER, R. Sensitivity analyses of gas release from a L/ILW repository in the Opalinus Clay including the microbial consumption of hydrogen. Nagra Arb. Ber. NAB 16-07. Nagra, Wettingen, Switzerland, 2016.
[8] PRUESS, K., OLDENBURG, C., MORIDIS, G. TOUGH2 user's guide, Version 2. Lawrence Berkeley Laboratories, Report LBL-43134, Berkeley, USA, 1999.
[9] LEUPIN, O., SMITH, P., SAVAGE, D., JOHNSON, L., MARSCHALL, P., SCHNEIDER, J. & SENGER, R. High-level waste repository-induced effects. Nagra Tech. Rep. NTB 14-13. Nagra, Wettingen, Switzerland, 2016.
[10] LEUPIN, O., SMITH, P., SAVAGE, D., JOHNSON, L., MARSCHALL, P., SCHNEIDER, J. & SENGER, R. Low- and intermediate-level waste repository-induced effects. Nagra Tech. Rep. NTB 14-13. Nagra, Wettingen, Switzerland, 2016.
[11] MARSCHALL, P., SMITH, P., PAPAFOTIOU, A., LI, C., NAMHATA, A. E3-HP-LBE: Preliminary assessment of RIE indicators for Dry Run (HP-SV). Nagra Technical Note AN 18-044. Nagra, Wettingen, Switzerland, 2018.
[12] NAGRA, SGT Etappe 2: Vorschlag weiter zu untersuchender geologischer Standortgebiete mit zugehörigen Standortarealen für die Oberflächenanlage. Geologische Grundlagen. Nagra Tech. Rep. NTB 14-02. Nagra, Wettingen, Switzerland, 2014.
[13] NAGRA, Beurteilung der geologischen Unterlagen für die provisorischen Sicherheits-analysen in SGT Etappe 2. Nagra Technischer Bericht NTB 10-01. Nagra, Wettingen, Switzerland, 2010.
[14] JOHNSON, L.H., NIEMEYER, M., KLUBERTANZ, G., SIEGEL, P.& GRIBI, P. Calculations of the Temperature Evolution of a Repository for Spent Fuel, Vitrified High-level Waste and Intermediate Level Waste in Opalinus Clay. Nagra Technical Report NTB 01-04. Nagra, Wettingen, Switzerland, 2002.
[15] PAPAFOTIOU, A., SENGER, R. Thermo-hydraulic modelling of the temperature distribution in the siting region Nördlich Lägern. Nagra Arb. Ber. NAB 13-56. Nagra, Wettingen, Switzerland, 2013.
[16] PAPAFOTIOU, A., SENGER, R. Thermo-hydraulic modelling of the temperature distribution in the siting region Zürich Nordost and Südranden. Nagra Arb. Ber. NAB 13-57. Nagra, Wettingen, Switzerland, 2013.
[17] PAPAFOTIOU, A., SENGER, R. Thermo-hydraulic modelling of the temperature distribution in the siting region Jura Ost. Nagra Arb. Ber. NAB 14-39. Nagra, Wettingen, Switzerland, 2013.
[18] SENGER, R., PAPAFOTIOU, A., MARSCHALL, P. Gas related property distributions in the proposed host rock formations of the candidate siting regions in Northern Switzerland and in the Helvetic Zone. Nagra Arb. Ber. NAB 13-83. Nagra, Wettingen, Switzerland, 2013.
[19] PAPAFOTIOU, A., NAMHATA, A. Model-based assessment of repository induced effects in the vicinity of repositories for SF/HLW/ILW and L/ILW: Model portfolio for Dry-Run. Nagra Int. Ber. NIB 17-27. Nagra, Wettingen, Switzerland, 2017.
[20] SENGER, R., PAPAFOTIOU, A., MARSCHALL, P. Thermo-hydraulic simulations of the near-field of a SF/HLW repository during early- and late-time post-closure period. Nagra Arb. Ber. NAB 14-11, Wettingen, Switzerland, 2014.
[21] POLLER, A., MAYER, G., DARCIS, M., SMITH, P. Modelling of Gas Generation in Deep Geological Repositories after Closure. Nagra Tech. Rep. NTB 16-04. Nagra, Wettingen, Switzerland, 2016.
[22] NAGRA, Modellhaftes Inventar für radioaktive Materialien MIRAM 12. Nagra Arbeitsbericht NAB 13-39. Nagra, Wettingen, Switzerland, 2013.
[23] PAPAFOTIOU, A., A. NAMHATA, A. SINGH, M. WILLIAMS, M. JIGMOND, MARSCHALL, P. Parametric sensitivity analysis of heat and gas release from a geological repository for SF/HLW in northern Switzerland. Nagra NAB 17-05. Nagra, Wettingen, Switzerland, 2017.